Chemical Science

ROYAL SOCIETY OF CHEMISTRY

EDGE ARTICLE

View Article Online
View Journal | View Issue

Cite this: *Chem. Sci.*, 2021, **12**, 4850

All publication charges for this article have been paid for by the Royal Society of Chemistry

Received 3rd December 2020
Accepted 9th February 2021

DOI: 10.1039/d0sc06628a

rsc.li/chemical-science

Electrophilic reactivities of cyclic enones and α,β-unsaturated lactones†

Robert J. Mayer, [a] Patrick W. A. Allihn, [b] Nathalie Hampel,[a] Peter Mayer,[a] Stephan A. Sieber [b] and Armin R. Ofial [*a]

The reactivities of cyclic enones and α,β-unsaturated lactones were characterized by following the kinetics of their reactions with colored carbon-centered reference nucleophiles in DMSO at 20 °C. The experimentally determined second-order rate constants k_2 were analyzed with the Mayr–Patz equation, $\lg k = s_N(N + E)$, to furnish the electrophilicity descriptors E for the Michael acceptors. Cyclic enones and lactones show different reactivity trends than their acyclic analogs. While cyclization reduces the reactivity of enones slightly, α,β-unsaturated lactones are significantly more reactive Michael acceptors than analogously substituted open-chain esters. The observed reactivity trends were rationalized through quantum-chemically calculated Gibbs energy profiles (at the SMD(DMSO)/M06-2X/6-31+G(d,p) level of theory) and distortion interaction analysis for the reactions of the cyclic Michael acceptors with a sulfonium ylide. The electrophilicities of simplified electrophilic fragments reflect the general reactivity pattern of structurally more complex terpene-derived cyclic enones and sesquiterpene lactones, such as parthenolide.

Introduction

Cyclic carbonyl compounds with α,β-unsaturated positions are important motifs within many natural products (Chart 1).[1–3] Previous studies of their cellular reactivities with endogenous proteins revealed intriguing insights into their target profiles.[4,5] The ability of these biomolecules to react as electrophiles with nucleophilic sites furnishes them with a multitude of biological functions,[6,7] *e.g.* the recently reported inhibition of focal adhesion kinase 1 by parthenolide,[5a,b] the cytotoxic activity of dehydroleucodine against human leukemia cells,[8] or the ability of nimbolide to inhibit metastasis.[5c] Nature has structurally tailored the reactivity of α,β-unsaturated cyclic carbonyl compounds in different variants. In particular, α-methylene-γ-butyrolactones exhibit superior cellular protein binding compared to lactones with endocyclic π-system, likely associated with an elevated reactivity.[4a,9] For the sesquiterpene lactones costunolide and dehydrocostus lactone,[10] α,β-unsaturated δ-lactones such as leptomycin, fostriecin or the anguinomycins,[11–15] as well as for simple fragments, such as tulipalin A,[16] it has been analyzed that their biological activities mainly depend on the ability to alkylate biomacromolecules through Michael additions. Sometimes these Michael additions are coupled with subsequent steps to achieve irreversible covalent enzyme inhibition.[15] On the other hand, in modified rugulactones the α,β-unsaturated δ-lactone unit does not

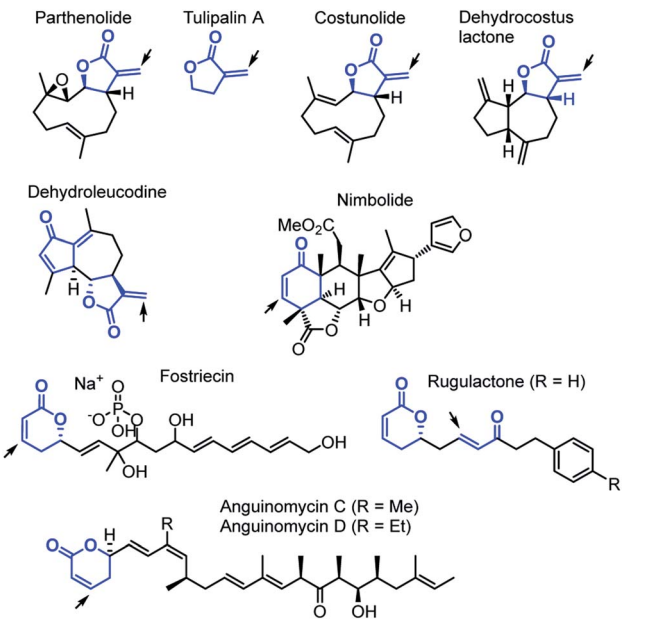

Chart 1 Examples for electrophilic natural products.

[a]*Department Chemie, Ludwig-Maximilians-Universität München, Butenandtstr. 5-13, 81377 München, Germany. E-mail: ofial@lmu.de*

[b]*Department Chemie, Technische Universität München, Lichtenbergstraße 4, 85748 Garching, Germany*

† Electronic supplementary information (ESI) available: Details of synthetic procedures and product characterization, kinetic measurements, quantum-chemical calculations, geometries of all optimized structures and X-ray crystallographic data. CCDC 2044215–2044221. For ESI and crystallographic data in CIF or other electronic format see DOI: 10.1039/d0sc06628a

contribute to the antibacterial effects and bioactivities of rugulactone were instead assigned to the reactivity of the α,β-unsaturated ketone unit.[17]

Despite these insights into proteome reactivity, a systematic analysis of the individual electrophilicity of the Michael acceptor moieties in different natural products or their truncated analogs is lacking. Knowledge of the reactivity of such biologically occurring electrophilic fragments would facilitate the identification of pharmacophores and is, therefore, of fundamental interest in biochemistry, toxicology, medicinal chemistry, and drug discovery.[9,18] Moreover, Michael acceptors with endo- and exocyclic unsaturation are also a structural motif of significant importance for synthetic chemists.[3]

In life-sciences, rate constants for the reactions of electrophiles with glutathione (GSH) are frequently used for estimating the reactivity and potential toxicity of various electrophilic compounds.[19–23] However, the most comprehensive overview of polar organic reactivity is currently given by Mayr and co-workers who used eqn (1) to characterize the reactivities of more than 1200 nucleophiles and over 300 electrophiles in solution phase.[24]

$$\lg k_2(20\ ^\circ\mathrm{C}) = s_\mathrm{N}(N + E) \quad (1)$$

Eqn (1) is a linear free energy relationship that allows for the semi-quantitative prediction of second-order rate constants k_2 for the reactions of electrophiles with nucleophiles from three parameters: the electrophilicity parameter E and the solvent-dependent nucleophilicity parameters N and s_N (susceptibility).

Recently, we determined the nucleophilic reactivity parameters N and s_N of GSH in aqueous solution, which facilitates to interconnect both approaches. Bioassay-derived GSH kinetics can now be used to roughly estimate Mayr electrophilicity parameters E, and *vice versa*. In this way, Mayr electrophilicities E for more than 70 acyclic Michael acceptors were estimated based on their previously determined kinetics toward GSH.[25] More precise electrophilicities E for a series of structurally simple acyclic Michael acceptors were determined from the kinetics of their reactions with carbon-centered one-bond nucleophiles (reference nucleophiles), that is, mainly with pyridinium and sulfonium ylides.[26,27]

We now set out to determine the Mayr electrophilicity parameters E of cyclic enones **1–3** and α,β-unsaturated lactones **4–5** by studying the kinetics of their reactions with the reference nucleophiles **6–7** (Chart 2). We then tested whether the Mayr E parameters obtained for the electrophilic core structures **1–5** are also representative of the reactivity profile of structurally more complex natural products that bear these fragments in their molecular scaffold. Quantum-chemical calculations were used to rationalize the observed reactivity trends which significantly differ from those for analogous acyclic (open chain) ketones and esters.

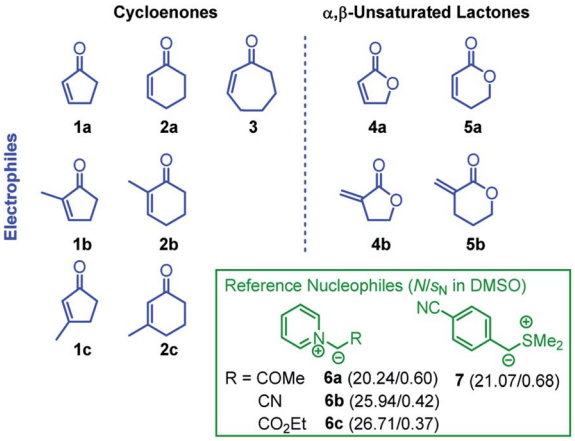

Chart 2 Electrophiles and reference nucleophiles used in this work.

Results and discussion

Product studies

The formal 1,3-dipolar cycloadditions (Huisgen reactions) of simple electron-deficient alkenes with pyridinium ylides, generated from *N*-alkylated pyridinium salts under basic conditions, are well-known to yield tetrahydroindolizines. Subsequent oxidation (*e.g.* with air or chloranil) efficiently aromatizes the newly formed heterocycles to afford diversely substituted indolizines.[27–31] In contrast, formation of the analogous tricyclic cyclopenta-, cyclohexa-, or cyclohepta-indolizines has rarely been studied. Only Tamura reported the formation of cyclohexaindolizines in low yield (10%) in a vinylic substitution reaction that used the pyridinium ylide **6c** (R = CO_2Et) and 3-chlorocyclohexanone as educts.[32] Direct 1,3-dipolar cycloaddition reactions of pyridinium ylides with cyclic enones or α,β-unsaturated lactones have not been reported to the best of our knowledge.

We planned to use the pyridinium ylides **6** as colored reference nucleophiles to follow the kinetics of their reactions with cyclic Michael acceptors by photometric methods. Given the lack of knowledge about the outcome of these reactions, we decided to characterize the products of a subset of the electrophile/nucleophile combinations under the conditions of the kinetic experiments, that is, in DMSO at 20 °C (Scheme 1).

Treatment of a 1 : 1-mixture of the pyridinium salt **6b**·HY (HY = HCl, HBr) and sodium carbonate with a DMSO solution of cyclopentenone (**1a**, 2 equiv.) resulted in a (3+2)-cycloaddition to give a mixture of diastereomeric tetrahydroindolizines. Due to their high sensitivity toward oxidation[33] and to facilitate the product purification, we oxidized these initial adducts to the aromatic indolizine **8**, which was isolated in 18% yield and characterized by single-crystal X-ray diffraction. We were delighted to find that analogous reactions of **6b** with cyclohexenone (**2a**), cycloheptenone (**3**) as well as with the lactone **5a** gave the corresponding indolizines **9b**, **10**, and **11**, respectively, in significantly higher yields (72–86% of isolated products). Furthermore, cyclohexaindolizines **9a** and **9c** were isolated in high yields from the reactions of the ester- and keto-stabilized pyridinium ylides **6a** and **6c** with cyclohexenone (**2a**).

To diversify the types of reference nucleophiles in our kinetic studies, we also investigated the reactions of the cyclic electrophiles with the sulfonium ylide **7**. Treatment of a solution of the sulfonium tetrafluoroborate **7**·HBF_4 and a cyclic Michael

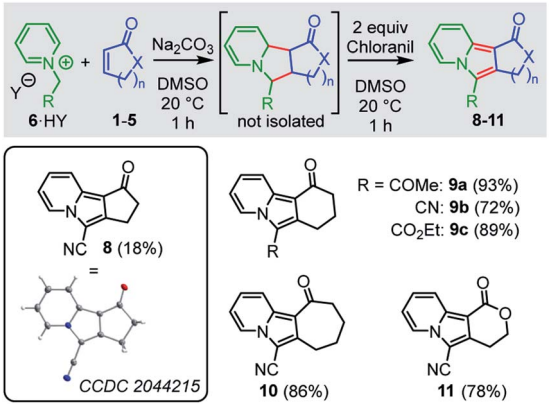

Scheme 1 Products for the reactions of the pyridinium ylides **6** (generated by deprotonation of **6**·HY) with cyclic Michael acceptors (yields of isolated products after chromatography, see ESI† for details). Insert: Single-crystal X-ray structure of **8**. Thermal ellipsoids drawn at a 50% probability level.

acceptor in DMSO with potassium *tert*-butoxide generated the sulfonium ylide **7** which then underwent cyclopropanation reactions with the electrophiles **1a**, **2a**, **4a**, and **5a** (Scheme 2). The cyclopropanes **12–15** were obtained as mixtures of diastereomers. Separation of the diastereomers by column chromatography was not always possible. However, purified diastereomers of **12** and **15** could be crystallized and characterized by single-crystal X-ray crystallography, providing unequivocal evidence for the cyclopropanation reaction.

The lactones **4b** and **5b** reacted with the sulfonium ylide **7** at their *exo*-methylene groups to give diastereomeric mixtures of **16** (46%) and **17** (69%), respectively. Owing to their sufficiently different polarity these diastereomeric mixtures were separable by column chromatography. One diastereomer of **16** and one of **17** were crystallized and analyzed by single-crystal X-ray diffraction (Scheme 2).

As a general trend, the yields of the cyclopropanes **12–17** depended on two factors: (a) the excess and (b) the absolute concentration of the electrophiles. A survey of the reaction conditions showed that highest yields were obtained when the cyclic Michael acceptor was present in excess (up to 10 equiv.) over the pronucleophile **7** and/or at low concentrations (<0.01 M). Experimental protocols with higher concentrations of the Michael acceptors or reduced excess (1.5 equiv.) resulted in complete consumption of the colored ylide **7**, too, but the cyclopropanes were only formed as minor products under these conditions. Instead, **7** isomerized in a background reaction to furnish the sulfide **18**,[34,35] presumably through a Sommelet–Hauser type of rearrangement (Scheme 3).[36]

The sulfide **18** is the starting material for BAY 85-8501, a candidate for the treatment of inflammatory diseases such as acute lung injury.[35] We characterized **18** by single-crystal X-ray diffraction. Solutions with low concentrations of **7** in DMSO isomerized slower ($t_{1/2}$ = 30 min at $[7]_0 = 1 \times 10^{-4}$ M) than solutions with higher concentrations of **7** ($t_{1/2}$ = 4 min at $[7]_0$ = 0.057 M, monitored by time-resolved ^{1}H NMR spectroscopy). Thus, the isomerization of **7** into **18** partially consumed the

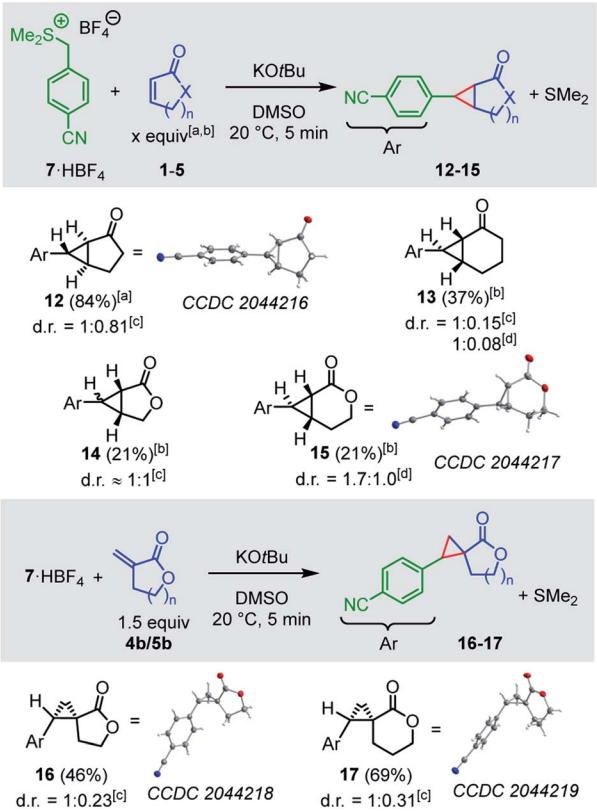

Scheme 2 Products for the reactions of the sulfonium ylide **7** with the electrophiles **1–5** (yields of isolated products after column chromatography, thermal ellipsoids drawn at 50% probability level, see ESI† for details). [a] 5 equiv., [b] 10 equiv., [c] d.r. determined after extraction, [d] d.r. determined after column chromatography.

nucleophile when **7** was combined with weakly or only moderately reactive electrophiles, whose cyclopropanations proceeded at comparable time scale as the Sommelet–Hauser rearrangement of **7**.

Kinetics

The kinetics of the reactions of the colorless electrophiles **1–5** with the pyridinium (**6**) and sulfonium (**7**) ylides were determined by following the decay of the UV-vis absorbance of the colored nucleophiles. Reactions at the seconds to minutes timescale were followed by conventional photometry. Stopped-flow photometric methods were employed for faster reactions in the millisecond regime. DMSO was used as the solvent for all

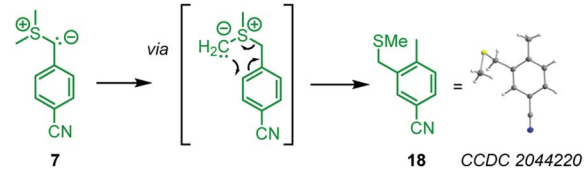

Scheme 3 Isomerization of the sulfonium ylide **7** to the benzyl methyl sulfide **18** (thermal ellipsoids drawn at 50% probability level).

electrophile–nucleophile combinations, which were uniformly studied at 20 °C.

Solutions of the ylides **6** and **7** in DMSO were generated by adding stoichiometric amounts of potassium *tert*-butoxide to the corresponding pyridinium or sulfonium salts. In the next step, these DMSO solutions were mixed with an excess (>10 equiv.) of the electrophiles **1–5**. With this ratio of reactants, the concentration of the excess compound can be assumed to remain practically constant during the kinetic measurements, which simplifies the kinetics and makes it possible to determine rate constants k_{obs} under pseudo-first order conditions. In general, the time-dependent change of the nucleophile's absorbance followed a mono-exponential decay. The first-order rate constants k_{obs} were then determined by a least-squares fitting of the mono-exponential decay function $A_t = A_0 \exp(-k_{obs} \times t) + C$ to the experimental absorbances A_t (Fig. 1A).

The correlation of k_{obs} with the concentration of the electrophiles **1–5** revealed a linear relationship, the slope of which corresponds to the second-order rate constant k_2^{exp} (Fig. 1B, Table 1). Isomerization (of **7**) and/or decomposition of the colored reference nucleophiles proceed concurrently and impede the kinetic study of slower reactions. Therefore, only the highly reactive nucleophile **6c** was available to study the rather unreactive 2- and 3-methylated cyclic enones **1c**, **2b**, and **2c**.

Based on the set of experimental second-order rate constants k_2^{exp}, we calculated the electrophilicity parameters E for compounds **1–5** by applying eqn (1) and the reported Mayr nucleophilicity parameters N and s_N of the reference nucleophiles.[24d,30,37]

Electrophilicity of natural products

Natural products. Cyclic Michael acceptors are frequent moieties in natural products (NPs), such as sesquiterpene lactones.[13,14] We, therefore, set out to assess whether the electrophilicity parameters determined for the simple cyclic Michael acceptors **1–5** (Chart 2) also hold to estimate the correct order of reactivity for analogous, but more complex, natural products. We made use of the reference nucleophiles **6c** and **7** to investigate the kinetics of their reactions with different classes of electrophilic natural products with embodied cyclic enone or *exo*-methylene lactone units (Chart 3). The monoterpenes carvone (**19**) and verbenone (**20**) as well as the sesquiterpene nootkatone (**21**) were used to test the reactivity of naturally occurring cyclic enones. Four sesquiterpene lactones (parthenolide **22**, costunolide **23**, dehydroleucodine **24**, dehydrocostus lactone **25**) were chosen to gain insight into the reactivity of *exo*-methylene lactones.

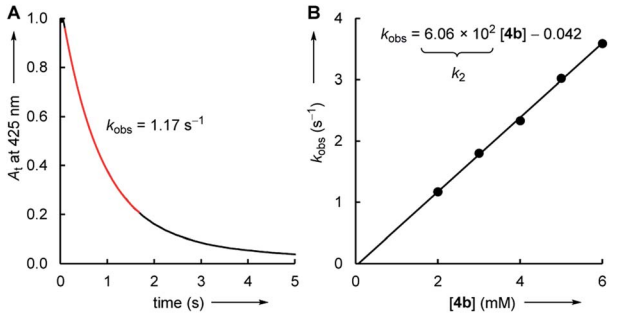

Fig. 1 (A) Decay of the ylide absorbance during the reaction of enone **4b** (2 mM) with pyridinium ylide **6c** (0.1 mM) in DMSO at 20 °C. (B) Plot of k_{obs} *versus* the concentration of **4b** for the determination of k_2^{exp}.

Product studies. ^{1}H NMR spectroscopic studies of the products of the reactions of the natural products **22–25** with the nucleophile **7** indicated exclusive cyclopropanation at the α-methylene lactone fragments. Neither was nucleophilic opening of the epoxide ring in parthenolide (**22**) nor cyclopropanation of the 3-methylcyclopentenone moiety in dehydroleucodine (**24**) observed. However, the cyclopropanations of **22–25** by **7** do not proceed with noticeable stereoselectivity and mixtures of up to four diastereomers were obtained, *e.g.* with dehydroleucodine (**24**). Luckily, the reaction of **7** with parthenolide (**22**) furnished a mixture of only two major diastereomeric products after separation by preparative thin layer chromatography, and single-crystal X-ray crystallography of **26** (arbitrarily taken from the diastereomeric mixture of crystalline material) corroborated the structural assignment on the fundament of our NMR spectroscopic analysis (Scheme 4).

Reactivity studies. Direct kinetic measurements in DMSO at 20 °C and the determination of second-order rate constants k_2 in analogy to those for the fragments **1–5** require access to sufficient quantities of the electrophilic reaction partner used in excess over the colored reference nucleophiles. The available quantities were sufficient to follow this strategy for the natural products **19–22**, and the kinetics of their reactions were studied toward the pyridinium ylide **6c** as reference nucleophile. The Mayr electrophilicities E of **19–22** (Table 2) were estimated by substituting the experimental second-order rate constants k_2^{exp} and the known N and s_N for **6c** in eqn (1).

Competition experiments were performed to estimate the Mayr electrophilicities E of the *exo*-methylene lactones **22–25** (= natural products, NP). The lactone **4b** ($E = -19.4$) was chosen as the competition partner because it contains the entire core structure of the electrophilic moiety in the natural products. As outlined in Scheme 5,[38] the experiments were performed such that the reference nucleophile **7** (generated in solution from **7**·HBF_4 with KO*t*Bu) was completely consumed in reactions with an excess of the two competing electrophiles NP and **4b**. Consequently, the product mixture contained the remaining electrophiles NP and **4b** as well as both products, the respective cyclopropanated natural product CNP (from NP + **7**) and **16** (from **4b** + **7**). The reaction mixture was analyzed by ^{1}H NMR spectroscopy to determine the competition constant κ according to eqn (3). The competition constants κ were then used to estimate the E parameters for the electrophilic NPs **22–25** (Table 2).

The reactivity of parthenolide (**22**) was characterized by both approaches. An electrophilicity $E = -19.0$ was determined from the direct kinetic measurements with **6c** and $E = -18.5$ resulted from the competition experiment (*vs.* **4b**) with the nucleophile **7**. Thus, the E values determined by the two different experimental methods agreed within one order of magnitude, and an

Table 1 Experimental and calculated second-order rate constants k_2 for the reactions of the Michael acceptors **1–5** with the reference nucleophiles **6–7** in DMSO at 20 °C

Electrophiles	Nucleophiles	k_2^{exp} (M^{-1} s^{-1})	$k_2^{eqn\ (1)}$ (M^{-1} s^{-1})	$k_2^{exp}/k_2^{eqn\ (1)}$
1a, $E = -20.6$[a]	**6a**	1.51 ± 0.05	6.1×10^{-1}	2.5
	7	1.06 ± 0.05	2.1	0.51
	6c	$(1.62 \pm 0.01) \times 10^{2}$	1.8×10^{2}	0.89
1b, $E = -22.1$[a]	**6a**	$(3.69 \pm 0.19) \times 10^{-2}$	7.7×10^{-2}	0.48
	7	1.05 ± 0.02	2.0×10^{-1}	5.3
	6c	7.83 ± 0.85	5.1×10^{1}	0.15
1c ($E = -28.9$)[a,b]	**6c**	$(1.55 \pm 0.18) \times 10^{-1}$	—	—
2a, $E = -22.1$[a]	**6a**	$(7.60 \pm 0.36) \times 10^{-2}$	7.7×10^{-2}	0.99
	7	$(5.16 \pm 0.12) \times 10^{-1}$	2.0×10^{-1}	2.6
	6c	$(1.07 \pm 0.01) \times 10^{1}$	5.1×10^{1}	0.21
2b ($E = -27.5$)[a,b]	**6c**	$(5.00 \pm 0.49) \times 10^{-1}$	—	—
2c ($E = -29.6$)[a,b]	**6c**	$(8.70 \pm 1.31) \times 10^{-2}$	—	—
3, $E = -22.0$[a]	**6a**	$(8.13 \pm 0.49) \times 10^{-2}$	8.8×10^{-2}	0.92
	7	$(5.31 \pm 0.17) \times 10^{-1}$	2.3×10^{-1}	2.3
	6c	$(1.19 \pm 0.05) \times 10^{1}$	5.5×10^{1}	0.22
4a, $E = -20.7$[a]	**6a**	$(4.14 \pm 0.10) \times 10^{-1}$	5.3×10^{-1}	0.78
	7	2.89 ± 0.16	1.8	1.6
	6c	$(8.09 \pm 0.02) \times 10^{1}$	1.7×10^{2}	0.48
4b, $E = -19.4$[a]	**6a**	5.47 ± 0.27	3.2	1.7
	7	8.39 ± 0.38	1.4×10^{1}	0.61
	6c	$(6.06 \pm 0.12) \times 10^{2}$	5.1×10^{2}	1.2
5a, $E = -21.8$[a]	**6a**	$(9.68 \pm 0.27) \times 10^{-2}$	1.2×10^{-1}	0.84
	7	$(4.12 \pm 0.08) \times 10^{-1}$	3.2×10^{-1}	1.3
5b, $E = -19.5$[a]	**6a**	6.62 ± 0.23	2.8	2.4
	7	5.10 ± 0.04	1.2×10^{1}	0.44
	6c	$(6.01 \pm 0.14) \times 10^{2}$	4.7×10^{2}	1.3

[a] This work. [b] Electrophilicity E estimated on the basis of only one rate constant k_2^{exp}.

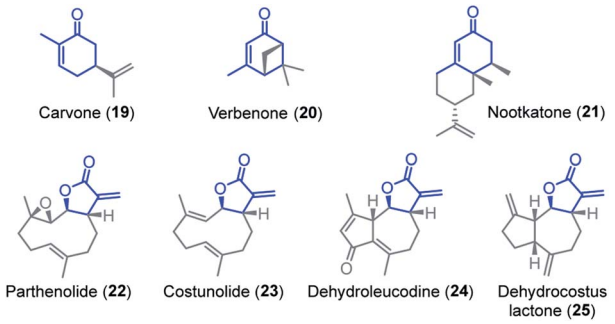

Chart 3 Electrophilic natural products (NPs).

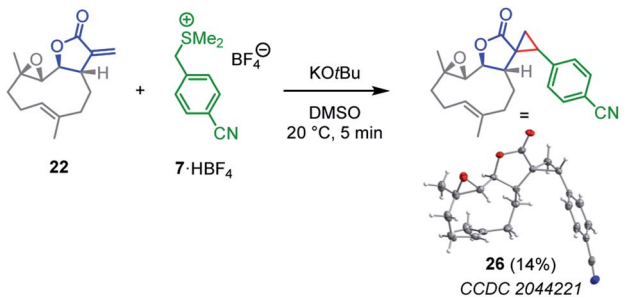

Scheme 4 Cyclopropanation of parthenolide (**22**) by the sulfonium ylide **7** (yield of isolated product after chromatographic workup, thermal ellipsoids drawn at 50% probability level, see ESI† for details).

Table 2 Experimental second-order rate constants or competition constants (*vs.* **4b**) for the reactions of natural products **19–25** with reference nucleophiles **6c** and **7** in DMSO at 20 °C

Electrophile (NP)	Nucleophile	$k_2^{exp,a}$ (M^{-1} s^{-1})	κ^b	Mayr E
19	**6c**	$(5.5 \pm 0.1) \times 10^{-1}$		−27.4
20	**6c**	$(8.3 \pm 1.2) \times 10^{-2}$		−29.6
21	**6c**	$(2.8 \pm 0.1) \times 10^{-2}$		−30.9
22	**6c**	$(7.3 \pm 0.3) \times 10^{2}$		−19.0
	7		4.4	(−18.5)[c], av −18.8
23	**7**		1.3	(−19.2)[c]
24	**7**		4.6	(−18.4)[c]
25	**7**		1.9	(−19.0)[c]

[a] Kinetics were determined photometrically by following the decay of the absorbance of the nucleophile **6c**. [b] Determined by competition experiments with **4b** as competition partner. [c] $E = E(\mathbf{4b}) + (\lg \kappa)/s_N(\mathbf{7})$.

averaged $E = -18.8$ is a realistic semiquantitative estimate for the electrophilicity of parthenolide (**22**).

Substituents remote from the electrophilic π-system have only a minor impact on the observed reactivity. Carvone (**19**) is almost as reactive as 2-methylcyclohexenone (**2b**) and verbenone (**20**) has a similar reactivity as 3-methylcyclohexenone (**2c**). Only a significant increase of the steric hindrance in the vicinity to the reaction center, for example in nootkatone (**21**), causes another slight decrease in electrophilicity in comparison with the model fragment **2c**.

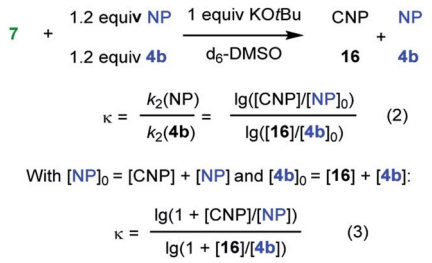

$$\kappa = \frac{k_2(\mathrm{NP})}{k_2(\mathbf{4b})} = \frac{\lg([\mathrm{CNP}]/[\mathrm{NP}]_0)}{\lg([\mathbf{16}]/[\mathbf{4b}]_0)} \quad (2)$$

With $[\mathrm{NP}]_0 = [\mathrm{CNP}] + [\mathrm{NP}]$ and $[\mathbf{4b}]_0 = [\mathbf{16}] + [\mathbf{4b}]$:

$$\kappa = \frac{\lg(1 + [\mathrm{CNP}]/[\mathrm{NP}])}{\lg(1 + [\mathbf{16}]/[\mathbf{4b}])} \quad (3)$$

Scheme 5 Outline of competition experiments (NP denotes a certain electrophile from the series **22–25** and CNP the respective cyclopropanation product formed upon reaction of NP with the nucleophile **7**).

Application of electrophilicity parameters in synthesis

The levels of electrophilicity derived from the ranking of **1–5** in the Mayr electrophilicity scale (Fig. 2) facilitate assessing the reaction times and experimental conditions required for successful reactions with C-nucleophiles (see comment box in Fig. 2).[24d] Usually, reactions with predicted second-order rate constants of $k_2 < 10^{-5}$ M^{-1} s^{-1} (at 20 °C) will need catalytic activation, heating or significantly extended reaction times to furnish products. In the subsequent summary, the reaction conditions of reported procedures are compared with predictions based on the Mayr–Patz eqn (1).

In accord with the determined electrophilicity, tulipalin A (**4b**, α-methylene-γ-butyrolactone, $E = -19.4$) was reported to undergo high yielding DBU-catalyzed Michael reactions with the nitromethane- ($N/s_N = 20.7/0.60$ in DMSO) (−25 to 20 °C, 16 h)[39] and 2-nitropropane-derived carbanions ($N/s_N = 20.6/0.69$ in DMSO) (20 °C, 48 h).[40] The Michael adduct from the reaction of **4b** with the deprotonated diethyl 2-chloromalonate ($N/s_N = 18.2/0.74$ in DMSO) (in THF, r.t., 6 h, 85% yield) was accompanied by traces of the corresponding 4-oxo-5-oxaspiro[2,4] heptane, generated *via* a cyclopropanation reaction. This sequence of nucleophilic attack at **4b** with subsequent ring closure was exclusively observed when diethyl 2-bromomalonate was used as the pronucleophile in the analogous reaction with **4b** (in THF, r.t., 10 h, 75% yield).[41] Furthermore, the piperidine-catalyzed Michael addition of malononitrile ($N/s_N = 18.2/0.69$ in MeOH) at **4b** was reported to be facile at ambient temperature in ethanol. The reaction did not stop at the 1 : 1 stage and furnished the two-fold alkylated malononitrile (piperidine cat, EtOH, 2–3 min, product precipitates, 75% yield).[42] The carbon–carbon bond-formation between **4b** and the weakly nucleophilic Meldrum's acid-derived enolate ion ($N/s_N = 13.9/0.86$ in DMSO) is predicted by eqn (1) to be very slow at 20 °C ($k_2^{\mathrm{eqn\ (1)}} = 4 \times 10^{-7}$ M^{-1} s^{-1}), and effective product formation required phase transfer catalysis and elevated reaction temperatures (TEBA–Cl in MeCN, 50 °C, 10 h, 64% yield).[43] Reactions of dehydrocostus lactone (**25**, $E = -19.0$) with the anion of nitromethane ($N/s_N = 20.7/0.60$ in DMSO, 90% yield) were carried out under the same experimental conditions as applied for **4b**, the core electrophilic fragment of **25**.[39]

Given the almost identical electrophilic reactivities, it is unsurprising that reported Michael additions or cyclopropanation reactions of α-methylene-pyranone (**5b**, $E = -19.5$) cover the same spectrum of carbon-nucleophiles as for **4b**. Carbanions generated by deprotonation of diethyl 2-chloro- and 2-bromomalonate (for 2-Br-malonate: in THF, r.t., 10 h, 85% yield)[41] and 2-nitropropane (DBU-catalyzed in MeCN, r.t., 4.5 h, 81% yield)[44] were successfully used to functionalize **5b**.

Michael additions of nitroethane to cyclopentenone (**1a**, $E = -20.6$) and cyclohexenone (**2a**, $E = -22.1$) under basic conditions were reported.[45] Enantioselective additions of the anion generated by deprotonation of dimethyl malonate ($N/s_N = 20.2/0.65$ in DMSO) to **1a** were carried out in the presence of a bifunctional amine-thiourea catalysts (toluene, 50 °C, 20 h, 84% yield).[46] Alkylations of the cyclic enones **1a**, **2a**, and **3** ($E = -22.0$) at their β-positions were also reported when dimethyl malonate was deprotonated by potassium *tert*-butoxide (in THF, r.t., 92–95% yield)[47a] or when **3** reacted with the slightly less reactive ethyl acetoacetate-derived carbanion (in ethanol, 25 °C, 21 h, 52% yield).[47b] Furthermore, the cyclic enones **1a** and **2a** were used as substrates for cyclopropanation reactions with the sulfonium ylide generated from trimethylsulfoxonium iodide ($N/s_N = 21.3/0.47$ in DMSO).[48] Elongated reaction times were needed (DBU, $CHCl_3$, r.t., overnight, 82% yield), however, when a bicyclic framework was constructed from cyclopentenone **1a** with the less nucleophilic sulfonium ylide derived from ethyl (dimethylsulfonium)acetate bromide ($N/s_N = 15.9/0.61$ in DMSO).[49]

With the same sulfonium ylide as the nucleophile, the butenolide **4a** ($E = -20.7$) was reported to produce only a poor yield (22%) of the attempted cyclopropanation product (Cs_2CO_3, DMF, r.t., reaction time not given).[50] Conjugate additions of silyl ketene acetals ($N/s_N = 9.0/0.98$ in CH_2Cl_2 for $Me_2C{=}C(OMe)OSiMe_3$) to **4a** and 5,6-dihydro-2*H*-pyran-2-one **5a** ($E = -21.8$) required activation *e.g.* by Lewis acid catalysts to be productive.[51]

The highly reactive phenyl lithium reacted with 2-methyl cyclohexenone (**2b**) through 1,2-addition at the carbon atom of the carbonyl group.[52] The electron-poor olefin **2b** ($E = -27.5$) underwent conjugate additions, however, with the anion of dimethyl malonate ($N/s_N = 18.2/0.64$ in MeOH) in methanol or ethanol after initial heating and long overall reaction times (MeOH, 16 h (ref. 53) and EtOH, 60 °C for 5 h + 20 °C, 12 h).[54] The Michael addition of nitroethane ($N/s_N = 21.5/0.62$ in DMSO) to **2b** was accomplished by deprotonation of the pronucleophile with *N*,*N*,*N*′,*N*′-tetramethylguanidine and stirring the acetonitrile solution for 3 days at ambient temperature (62% yield).[45] Analogous reactions of deprotonated nitroethane with the even less electrophilic 3-methylcycloalkenones **1c** ($E = -28.9$) and **2c** ($E = -29.6$) were carried out under phase transfer catalysis to avoid too long reaction times (K_2CO_3/TEBA–Cl in benzene, r.t. for 4 days, 51% yield from **1c**).[45]

Accordingly, **2c** ($E = -29.6$) requires a reaction time of 9 days for the Michael addition of the diethyl malonate-derived anion ($N/s_N = 18.2/0.64$ in MeOH) in ethanol at ambient temperature (74–76% yield).[55a] In an alternative procedure, the diethyl 2-methylmalonate-derived carbanion ($N/s_N = 21.1/0.68$ in DMSO) added to **2c** under 15 kbar pressure (DBN, MeCN, 45 °C, 36 h) in a yield of 50%.[55b]

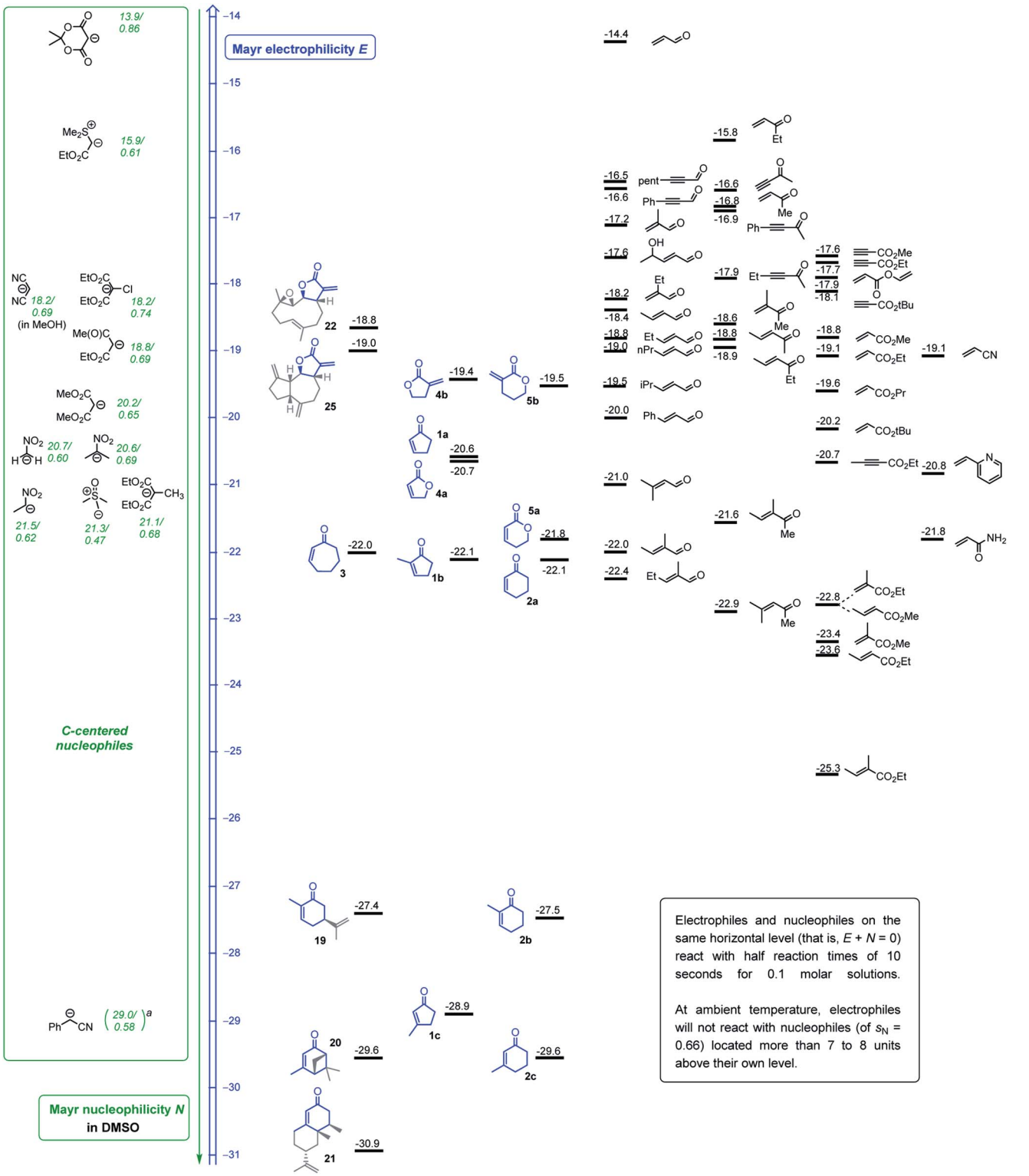

Fig. 2 Michael acceptors studied in this work (blue) or previously (ref. 25 and 27), ranked according to their electrophilicity parameters E and combined with a reactivity scale for C-centered nucleophiles (ordered by their N parameters, reactivity given as N/s_N). [a]Estimated N/s_N based on reactivity data for the carbanion derived from 2-phenylpropionitrile (ref. 24*d*).

The reaction of **2c** with the highly nucleophilic lithiated phenylacetonitrile ($N/s_N = 29.0/0.58$ in DMSO, estimated based on data for 2-phenylpropionitrile)[24d] delivers within a few minutes the allyl alcohols *via* kinetically controlled 1,2-addition (−90 °C in THF). The 1,2-addition is reversible, however, and extended reaction times or slightly higher temperatures furnish

the corresponding ketone *via* the thermodynamically favored 1,4-attack (THF, −60 °C, 120 min, 95%).[56]

This survey of reported reactions of C-nucleophiles with the cyclic Michael acceptors characterized in this work shows, that the determined Mayr electrophilicities *E* for the electrophiles **1–5** and the dehydrocostus lactone (**25**) are well in accord with practical experience in organic synthesis.

Structure reactivity relationships. Embedding the cyclic electrophiles **1–5** and electrophilic natural products **19–25** in the Mayr electrophilicity scale makes it possible to compare their reactivities with those of acyclic Michael acceptors (Fig. 2). The analysis in Fig. 3 reveals that cyclization changes the reactivity of enones and α,β-unsaturated esters in a way that is difficult to predict by intuition. Cyclic enones are by 2–3 *E* units weaker electrophiles than acyclic β-substituted enones. The opposite trend is observed for lactones: α,β-unsaturated lactones **4–5** are more reactive by 2–3 *E* units compared to their acyclic counterparts. We performed quantum-chemical calculations to rationalize these antipodal reactivity trends.

Quantum chemical calculations

Energy profiles. To gain further insight into the observed reactivity ranking and structural factors that influence the observed reactivity of cyclic Michael acceptors, we calculated the reaction profiles for the addition of the sulfonium ylide **7** to the electrophiles **1–5** at the SMD(DMSO)/M06-2X/6-31+G(d,p) level of theory using the Gaussian software package.[57]

As depicted in Fig. 4 for the reaction of **7** with cyclopentenone **1a**, zwitterionic intermediates **IM** are generated in the first step of the reaction mechanism (*via* **TS1**). The newly formed C–C bond connects two stereocenters, and the reaction can proceed through a *cis*- and a *trans*-attack. As displayed in Table 3, the computational results indicate that the *trans*-attack is slightly favored over the *cis*-attack for the cyclic Michael acceptors, except for the 2- and 3-methyl substituted electrophiles **1b**, **2b** and **2c**. In general, however, the computed differences between the *cis*- and the *trans*-pathways are small, in accord with the experimental observation that mixtures of diastereomeric products were isolated in moderate yields (Scheme 2). Hence, we refrained from interpreting the stereoselectivity of the cyclopropanation reactions and used the most favorable pathway for our subsequent analyses (if not stated otherwise).

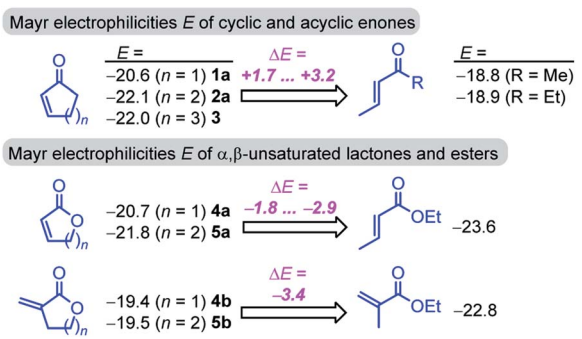

Fig. 3 Comparison of the Mayr electrophilicity parameters *E* for cyclic (from Table 1) and acyclic (from ref. 25 and 27) Michael acceptors.

In the final step, an intramolecular S_N2 reaction eliminates dimethyl sulfide from **IM** *via* **TS2** to yield the highly exergonic products, namely, dimethyl sulfide and cyclopropanes with *cis*- or *trans*-configuration. For all entries in Table 3, the relative Gibbs activation energies for **TS1** and **TS2** indicate that the addition (*via* **TS1**) is the rate-determining step in the reactions of **7** with **1a**.

As shown in Table 3 and graphically in Fig. 5A, the quantum-chemically calculated activation barriers $\Delta G^{\ddagger}$(**TS1**) agree reasonably well (±11 kJ mol^{-1}; mean deviation: ±3.3 kJ mol^{-1}) with the experimental $\Delta G^{\ddagger}$ determined either by experiment (k_2^{exp}) or by utilizing eqn (1) ($k_2^{eqn\ (1)}$). Accordingly, there is also a reasonable correlation of $\Delta G^{\ddagger}$(**TS1**) with the electrophilicity parameters *E* from Table 1 (Fig. 5B).

Enone conformation. If compared to analogous acyclic Michael acceptors, the cyclic enones studied in this work experience a significantly reduced conformational flexibility. Experimental electrophilicities were so far only determined for (*E*)-configured acyclic Michael acceptors. However, relevant information about the reactivity of (*Z*)-configured conformers, which is required for the discussion of stereoelectronic effects in cyclic enones, is missing. To get insights into the effects of locked conformations on transition state energetics, we set out to perform quantum-chemical calculations for the reaction of **7** with both (*E*)- and (*Z*)-pentenone.

As discussed by Bienvenüe on the basis of UV and IR spectroscopic data, (*E*)- and (*Z*)-enones exist in both the *s-trans* and *s-cis* form owing to the hindered rotation around the central carbon–carbon σ-bond (Fig. 6, top).[58] Experimental data[58] as well as computations (this work) agree that for (*E*)-pentenone both *s-cis* and *s-trans* conformers are of comparable energy. For (*Z*)-pentenone, however, the calculations indicate a significant preference for the *s-cis* form (*cis*/*trans* = 93 : 7). We then computed Gibbs energies for the transition states of the addition of **7** at both (*E*)- and (*Z*)-pentenone. We found that the *s-cis* conformers of (*E*)- and (*Z*)-pentenone both react with **7** *via* lower energy barriers than the respective *s-trans* conformers. As shown in Fig. 6 (bottom, left), the transition state energy for the *s-cis*-(*E*)-pentenone is 8.6 kJ mol^{-1} lower than that for the *s-trans*-(*E*)-conformer. The difference between the transition states for *s-trans*-(*Z*)- and *s-cis*-(*Z*)-pentenone amounts to 5.0 kJ mol^{-1} (Fig. 6, bottom, right). When the most favored transition states for (*E*)- and (*Z*)-pentenone are compared, the (*E*)-isomer of pentenone can be expected to be by approximately one order of magnitude more reactive than the (*Z*)-configured isomer ($\Delta\Delta G^{\ddagger}$ = 7.6 kJ mol^{-1}).

Furthermore, the calculations suggest that the experimentally characterized (*E*)-pentenone reacts *via* the *s-cis* transition state ($\Delta G^{\ddagger}$ = 69.7 kJ mol^{-1}) with nucleophiles (such as **7**). Conformationally locked cyclic species, such as **1a** or **2a**, adopt transition states similar to the unfavorable *s-trans* pathway for (*Z*)-pentenone ($\Delta G^{\ddagger}$ = 82.3 kJ mol^{-1}). Thus, we can roughly estimate that cyclic enones are at minimum by two orders of magnitude less reactive than analogously substituted α,β-unsaturated open-chain ketones. The Mayr *E* values for (*E*)-pentenone (*E* = −18.8), cyclopentenone (**1a**, *E* = −20.6),

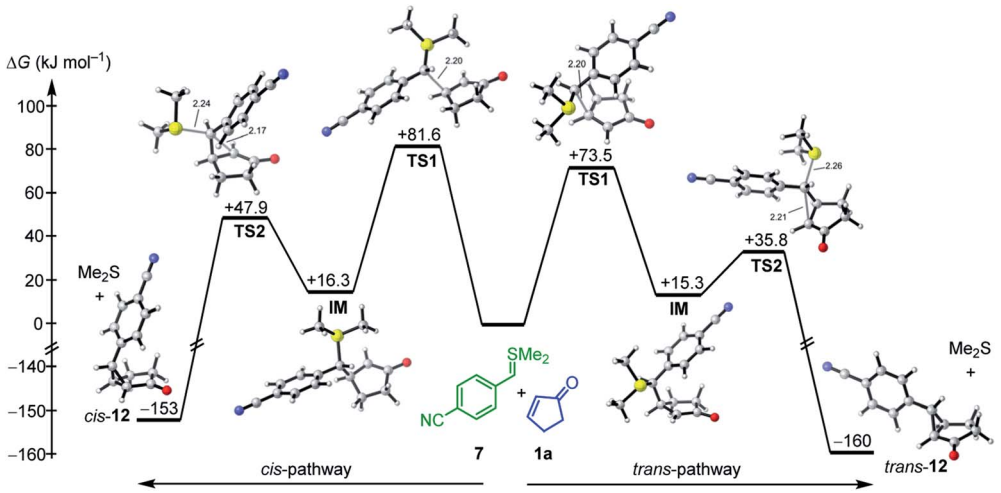

Fig. 4 Gibbs energy profile for the reaction of 7 with cyclopentenone (**1a**) at the SMD(DMSO)/M06-2X/6-31+G(d,p) level of theory (see ESI, Fig. S1,† for a distortion/interaction analysis).

cyclohexenone (**2a**, $E = -22.1$), and cycloheptenone (**3**, $E = -22.0$) are in acceptable accord with this naïve analysis.

Ester *vs.* lactone. Due to the analogous conjugated π-systems of unsaturated ketones and esters, (*E*/*Z*)-configurations and *s-cis*/*s-trans* conformations should influence the reactivity of esters in a similar manner as in ketones. Counterintuitively, (*Z*)-lactones are more electrophilic than their open-chain ester analogs with (*E*)-configured CC double bond (*cf.* Fig. 2), and other stereoelectronic effects seem to dominate their reactivity.

In line with the relative reactivity ranking in our work, lactones are well-known to undergo significantly faster alkaline hydrolysis than acyclic esters. This finding was explained by unfavorable orbital interactions in the transition state[59] or through differences in the dipole moments leading to ground state destabilization of (*Z*)-configured ester units.[60] More recently, stereoelectronic effects were suggested to explain the higher reactivity of unsaturated lactones.[61]

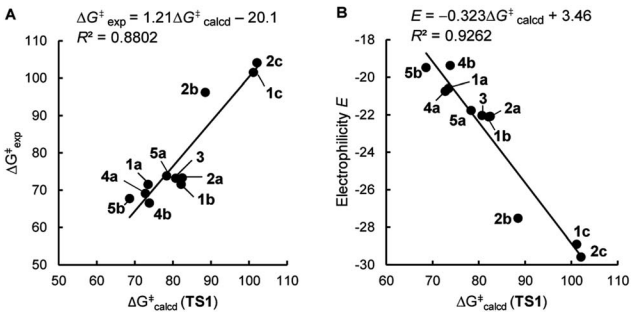

Fig. 5 Correlations of (A) experimental Gibbs activation energies $\Delta G^{\ddagger}_{exp}$ and (B) Mayr electrophilicity descriptors *E* with quantum-chemically calculated Gibbs activation barriers $\Delta G^{\ddagger}_{calcd}$(**TS1**) for the reactions of 7 with the electrophiles **1**–**5** at the SMD(DMSO)/M06-2X/6-31+G(d,p) level of theory ($\Delta G^{\ddagger}$ in kJ mol^{-1}).

Table 3 Quantum-chemically calculated energy profiles (in kJ mol^{-1}) for the addition of the sulfonium ylide 7 to the electrophiles **1**–**5** at the SMD(DMSO)/M06-2X/6-31+G(d,p) level of theory

				Trans-pathway				*Cis*-pathway			
Electrophiles	Mayr *E*	k_2 (M^{-1} s^{-1})	$\Delta G^{\ddagger}_{exp}$ [b]	$\Delta G^{\ddagger}$(**TS1**)[c]	ΔG°(**IM**)	$\Delta G^{\ddagger}$(**TS2**)	ΔG°	$\Delta G^{\ddagger}$(**TS1**)[c]	ΔG°(**IM**)	$\Delta G^{\ddagger}$(**TS2**)	ΔG°
1a	−20.6	1.1	71.5	**73.5**	15.3	35.8	−160.0	81.6	16.3	47.9	−152.7
1b	−22.1	1.1	71.6	83.7	28.8	51.1	−150.9	**82.1**	34.9	61.2	−144.3
1c	(−28.9)	4.7×10^{-6} [a]	101.7	**101.1**	46.7	66.8	−140.5	101.5	41.9	70.7	−137.7
2a	−22.1	0.52	73.4	**82.4**	19.2	42.9	−161.4	82.9	18.8	62.2	−145.0
2b	(−27.5)	4.1×10^{-5} [a]	96.4	92.4	42.9	54.8	−151.3	**88.5**	39.4	74.6	−139.7
2c	(−29.6)	1.6×10^{-6} [a]	104.3	103.4	46.3	70.0	−143.9	**102.1**	48.7	83.1	−133.1
3	−22.0	0.53	73.3	**80.7**	19.0	45.5	−172.8	85.8	12.4	56.7	−151.7
4a	−20.7	2.9	69.2	**72.8**	20.3	40.1	−159.5	79.9	17.7	56.8	−156.9
4b	−19.4	8.4	66.6	**73.8**	−1.0	24.8	−179.7	Ident.	Ident.	25.8	−179.3
5a	−21.8	0.41	73.9	**78.3**	15.0	44.3	−165.6	79.5	17.6	57.2	−153.3
5b	−19.5	5.1	67.8	**68.6**	−5.0	15.4	−176.0	Ident.	Ident.	24.0	−181.9

[a] k_2 calculated by using eqn (1), the nucleophilicity parameters *N* and s_N of 7 and the electrophilicity parameters *E* from Table 1. [b] Calculated by applying k_2 in the Eyring equation. [c] Entries for $\Delta G^{\ddagger}$(**TS1**) printed in bold indicate the favored transition state (*trans vs. cis*) used for the correlations in Fig. 5.

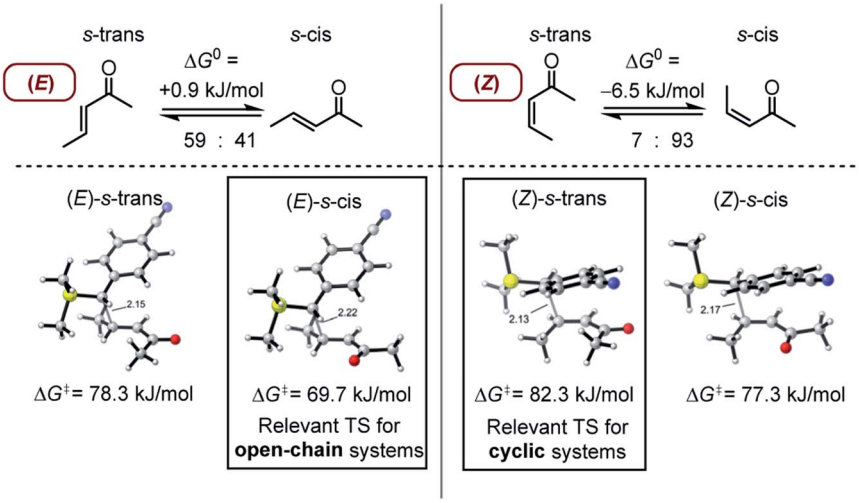

Fig. 6 Conformational equilibria and energetically lowest transition states for the reactions of **7** with the *s-cis* and *s-trans* conformers of (*E*)- and (*Z*)-pentenone at the SMD(DMSO)/M06-2X/6-31+G(d,p) level of theory.

For acyclic esters, the *s*-(*Z*) conformation is generally preferred, in which the n → σ* interaction donates electron density from the oxygen lone pair into the antiperiplanar antibonding σ^*_{CO} orbital (Fig. 7). This negative hyperconjugation reduces the electron-deficiency of the π-system and, in consequence, electrophilicity. In contrast, the locked *s*-(*E*) conformation in lactones impedes such a transfer of electron density and gives rise to an unattenuated electrophilic reactivity of the conjugated π-system (Fig. 7).[61]

The oxygen atom of the alkoxy group can affect the reactivity of the π-system only through a minor inductive effect. In line with this interpretation, the quantum-chemically calculated transition state structures for the addition of **7** at the ketone **2a** and the lactone **5a** are highly similar in geometry and energetics (Table 3, Fig. 8) in agreement with the almost identical experimentally determined second-order rate constants k_2^{exp} for both reactions (Table 1).

The unsaturated lactones **4b** and **5b** bearing an *exo*-methylene group are more electrophilic than the lactones **4a** and **5a** with endocyclic unsaturation. The higher reactivity can be attributed to the favorable interplay of two effects. First, the *s-trans* geometry is locked in lactones **4b** and **5b** in both the reactants and the transition states. Additionally, we assumed that the absence of substituents at the site of nucleophilic attack introduces less steric constraints in **4b**/**5b** than in **4a**/**5a**.

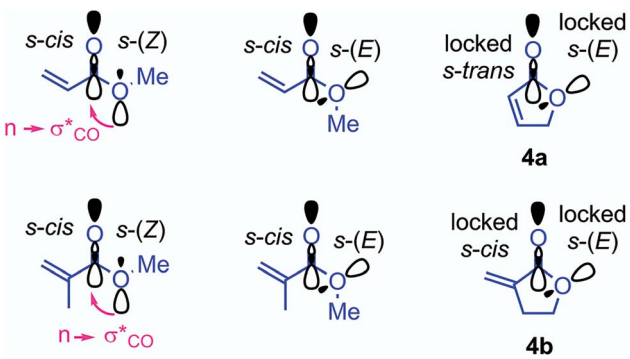

Fig. 7 Conformational dependency of the negative hyperconjugation in methyl (meth)acrylates and γ-butyrolactones.

To assess this hypothesis, a distortion interaction analysis (DIA)[62] was performed, which compared the transition states of the first step in the reactions of the S-ylide **7** with **2a**, **5a**, and **5b**, respectively (Fig. 8A). While the distortion energy of ylide **7** is identical in the reactions with **2a**, **5a** and **5b**, the distortion energy of the electrophile is significantly lower for **5b** than for **2a** or **5a**. It can be expected, that variable demand for geometrical changes at the electrophiles' reactive carbon atom upon C–C bond formation is key for the observed distortion energy difference in the comparison of **5b** *vs.* **5a**. We used the distance of the attacked C-atom of the electrophile from the plane defined by the three surrounding atoms in the transition state, as depicted in Fig. 8B, to describe the degree of pyramidalization Δ in the transition state. In line with Hine's principle of least nuclear motion (PLNM), which predicts 'that those elementary reactions will be favored that involve the least change in atomic position',[63] we observed a higher requirement for pyramidalization in the transition state of the reaction of **7** with **5a** (Δ = 0.227 Å, distortion energy: +39.7 kJ mol^{-1}) than in the analogous transition state for the faster reaction of **7** with **5b** (Δ = 0.174 Å, distortion energy: +34.3 kJ mol^{-1}).

Let's now analyze the higher interaction energy in the reaction of **7** with **5b** (−40.6 kJ mol^{-1}) than in the reaction of **7** with **5a** (−33.1 kJ mol^{-1}). It has previously been shown, that interaction energies can be further decomposed by energy decomposition analysis (EDA).[64] In this work, we applied symmetry-adapted perturbation theory (SAPT) at the sSAPT0/jun-cc-pVDZ level of theory, which decomposes an interaction into its electrostatic, exchange, induction, and dispersion components.[64] The SAPT analysis was performed in gas-phase with an entirely different theoretical method and, therefore, absolute numbers of the interaction energies differ from the results of our DFT

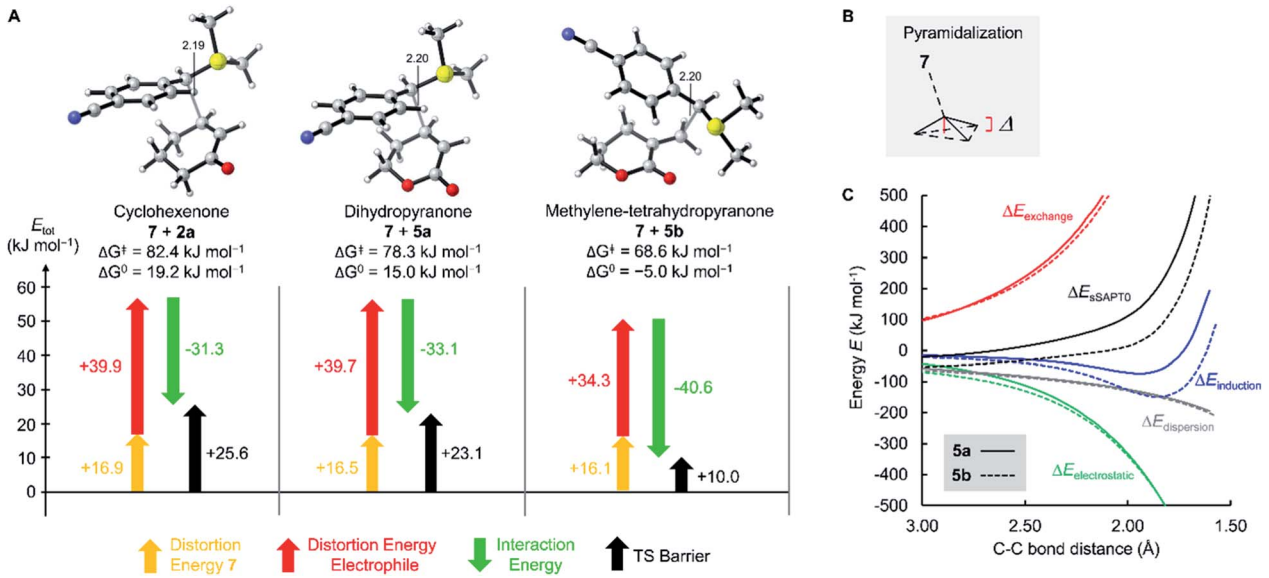

Fig. 8 (A) Distortion–interaction analysis at the transition state for the reactions of the sulfonium ylide 7 with **2a**, **5a** and **5b** at the SMD(DMSO)/M06-2X/6-31+G(d,p) level of theory. (B) Illustration of the pyramidalization Δ. (C) SAPT analysis for the reaction of 7 with **5a** and **5b**, respectively, at the sSAPT0/jun-cc-pVDZ level of theory in gas-phase.

method. Nevertheless, we expected the relative trends to hold. As shown in Fig. 8C, the interaction energy ($\Delta E_{\mathrm{sSAPT0}}$) for **5b** is generally more negative than for **5a**. Depending on the extent of bond formation, this is due to different origins. (1) During the approach to the transition state (located at 2.20 Å), it is the stronger electrostatic interaction that favors **5b** over **5a**. (2) At the transition state and in the further course of the reaction, however, the induction component becomes the decisive factor. In the transition state, the LUMO energy of the distorted **5b** is lower ($\varepsilon_{\mathrm{LUMO}} = -0.03527$ Hartree) than that of the distorted **5a** ($\varepsilon_{\mathrm{LUMO}} = -0.03309$ Hartree) while the HOMO energies of 7 are essentially identical (with **5b**: $\varepsilon_{\mathrm{HOMO}} = -0.21875$ Hartree; with **5a**: $\varepsilon_{\mathrm{HOMO}} = -0.21867$ Hartree). The smaller energetic gap for 7 + **5b** (4.99 eV) indicates a more favorable HOMO–LUMO interaction for the couple 7 + **5b** than for the combination 7 + **5a** (5.05 eV), in accord with the relative $\Delta E_{\mathrm{induction}}$ for **5b** and **5a** in the SAPT analysis.

Effects of 2- and 3-methyl substitution. Methyl substituents in the α- or β-position strongly influence the reactivity of enones. In a similar but more distinct way than in acyclic systems (Fig. 9A),[25,27] alkyl substitution of the C=C double bond drastically lowers electrophilicity of cyclic enones. A methyl group in the α-position reduces the electrophilicity E of cycloenones by 2 to 6 units (*cf.* Fig. 2). For substituents placed in the β-position this effect is even more pronounced: the reactivity of β-methyl cycloenones **1c** and **2c** is reduced by approximately 8 units on the Mayr E scale if compared to the unsubstituted analogs **1a** and **2a**, respectively. The retarding effect of α- and β-alkyl substituents at the cyclic enones may be caused by steric constraints and/or the electron donating ability of the alkyl group.

Again, DIA was used to quantify the effects. To keep the transition-state conformations comparable (Fig. 9B), the *trans*-TS for the reaction **1b** + 7 was evaluated in the DIA instead of the (by 1.6 kJ mol^{-1}) preferred *cis*-TS. As the C–C bond length in the transition state of the reaction **1a** + 7 differs from that of the reaction **1b** + 7, the entire pathways of the reactions of 7 with **1a**, **1b**, and **1c**, respectively, were analyzed. The positions of the distortion and interaction energy curves of **1c** (Fig. 9C) and **1b** (Fig. 9D) relative to those of **1a** reveal the reasons responsible for the reduced reactivity in both cases. Let us first discuss the effect of 3-substitution (Fig. 9C): the distortion energy for **1c** is significantly more positive than that for **1a** while the interaction energy is slightly more negative for **1c** than for **1a**.

As the C–C bond lengths in the transition states are similar for the reactions of 7 with the 3-substituted cycloenones and their unsubstituted analogs, these observations can also be assessed in a DIA of the respective transition state geometries of **1a** and **1c** (and analogously for **2a** and **2c**). As shown in Fig. 9E, the significant decrease of reactivity of β-substituted enones is mostly due to an increase of the distortion energy in both the enone fragments and the ylide 7. As previously discussed for **5a** and **5b**, pyramidalization Δ and Hine's PLNM can be utilized to rationalize the higher distortion energies of the 3-methyl substituted cycloenones. The reaction of **1a** with 7 requires a minor extent of pyramidalization ($\Delta = 0.222$ Å) than for the much less electrophilic **1c** ($\Delta = 0.303$ Å).[65] Moreover, the higher distortion energy of 7 in the reaction with **1c** than in that with **1a** can be rationalized by comparing the structures of the transition states (Fig. 9B). Different from the transition states for the reactions of 7 with **1a** or **1b**, the SMe_2 group of 7 is rotated in the transition state of the reaction with **1c** to avoid a clash with the methyl group of the electrophile.

Also 2-substituted cyclic enones were found to be weaker electrophiles than the unsubstituted analogs, though, for a different reason. The distortion energy curves for **1a**/**1b** (Fig. 9D) are highly similar or, for **2a**/**2b** (not depicted) even indicate a lower distortion component for **2b**. Hence, the

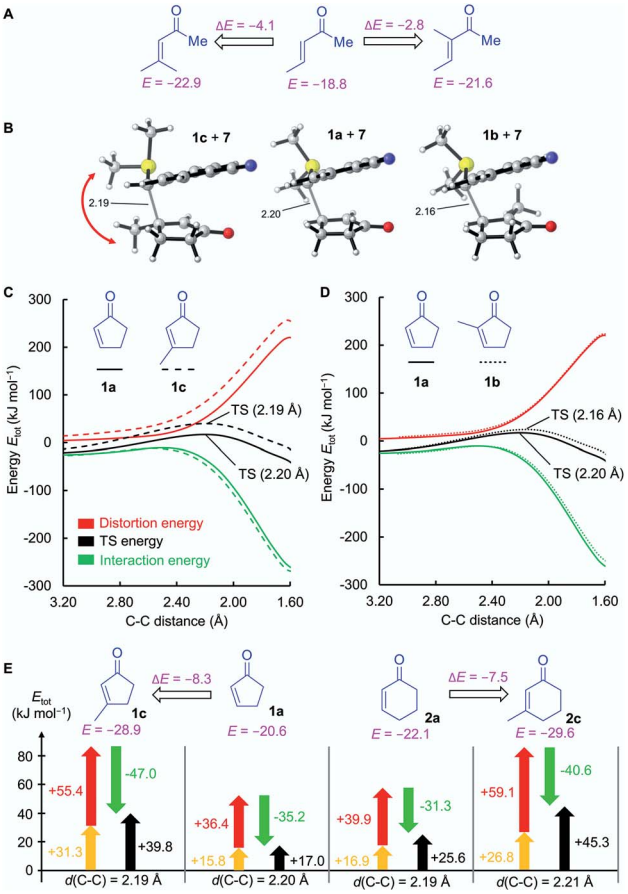

Fig. 9 (A) Reactivity trends for open-chain enones. (B) Structures of the *trans*-transition states for the reaction of **7** with the cyclopentenones **1a**, **1b**, and **1c** (the shown *trans*-TS for **1b** is by 1.6 kJ mol^{-1} higher in energy than the preferred *cis*-TS). (C) Distortion interaction analysis (SMD(DMSO)/M06-2X/6-31+G(d,p)) on the pathways of the reactions of **7** with **1a** and **1c**. (D) Distortion interaction analysis (SMD(DMSO)/M06-2X/6-31+G(d,p)) on the pathways of the reactions of **7** with **1a** and **1b**. (E) DIA of the transition states of the reaction of **7** with **1c**, **1a**, **2a** and **2c**. For the color legend of the DIA, see Fig. 8 (purple: Mayr electrophilicity descriptors *E*, black: electronic energies E_{tot}).

nucleophilic β-attack is not sterically hindered by the presence of an α-methyl group. However, the reaction path for **1b** suffers from a slightly less negative interaction energy than for the analogous reactions of **7** with **1a**.[66] Analysis of the involved HOMO/LUMO interactions of the fragments in the transition state resulted in a slightly stronger orbital interaction in the reaction of **7** with **1a** (5.14 eV) than in the reaction of **7** with **1b** (5.19 eV). Moreover, Hirshfeld atomic charge analysis of the fragments showed that in the transition state the reactive center of **1b** (+0.0391) is less positively charged than that of **1a** (+0.0472), presumably due to the electron-donating effect of the methyl group in **1b** (ESI, Fig. S3†).

Rate constants toward glutathione (GSH)

Helenalin is a sesquiterpene lactone isolated, *e.g.*, from *Arnica montana*, which embodies two different electrophilic units.[67] GSH was reported to attack faster, yet reversible,[67–69] at the cyclopentenone moiety of helenalin than at the α-methylene butyrolactone part.[68] This kinetic preference differs from the ordering of electrophilicities derived from our measurements, which predict higher reactivity for the unsaturated lactone from $E = -19.4$ for **4b** and $E = -20.6$ for **1a** (Fig. 10).

We, therefore, set out to evaluate whether the electrophilicity parameters *E* for the cyclic Michael acceptors, which we determined from their reactions with carbon-centered nucleophiles in DMSO solution, would enable us to also predict their reactivity toward glutathione (GSH) in aqueous solution. The rate constants for the reaction of GSH with the selected electrophiles were measured in aqueous, buffered solution at pH 7.4 by utilizing a modified bioassay.[19c,21b] An excess of the electrophile was added to an aqueous buffered (pH 7.4) solution of GSH. After certain time intervals, 5,5′-dithio-bis-(2-nitrobenzoic acid) (DTNB, Ellman's reagent) was added to allow for photometric quantification of unreacted GSH. The time dependent decay of the GSH concentration at 15–20 points was then evaluated by fitting a mono-exponential decay function, which furnished the first-order rate constants k_{obs} (s^{-1}). The kinetic procedure was repeated to collect k_{obs} at four different concentrations for each electrophile. The slope of the linear correlations of k_{obs} with the electrophile concentrations furnished the second-order rate constants k_{GSH} for the reactions of GSH with the cyclic Michael acceptors. Considering the small fraction of reactive thiolate GSH(NH_3^+/S^-) at pH 7.4 ($k_2^{exp} = k_{GSH}/F$, with $F = 0.028$ at pH 7.4)[25] finally converts k_{GSH} to k_2^{exp}.

The reactivity of glutathione GSH(NH_3^+/S^-) in aqueous solution has recently been rated with $N = 20.97$ ($s_N = 0.56$) on the Mayr nucleophilicity scale.[25] Thus eqn (1) was used to calculate $k_2^{eqn\ (1)}$ for the Michael addition of GSH(NH_3^+/S^-) with a set of cyclic unsaturated carbonyl compounds.

Typically, eqn (1) allows one to calculate second-order rate constants within a precision of factor <100 for reactions in which one new σ-bond is formed. Table 4 shows that eqn (1) estimated the second-order rate constants for the additions of GSH at cyclopentenone (**1a**), cyclohexenone (**2a**), the dihydropyranone **5a** and the α-methylene-pyranone **5b** within a factor of 20. For 2-methyl-cyclopentenone (**1b**) and the exo- and endocyclic lactones **4a** and **4b** k_2^{exp} and the calculated $k_2^{eqn\ (1)}$ agreed within a factor of 2. It can, thus, be concluded that the general reactivity pattern of cyclic electrophiles toward GSH is represented by their *E* parameters.

In agreement with previous studies by Schmidt on the dual electrophilicity of helenalin toward GSH,[67,68] we determined k_{GSH} (**1a**) > k_{GSH} (**4b**). Hence, we have to note that small reactivity

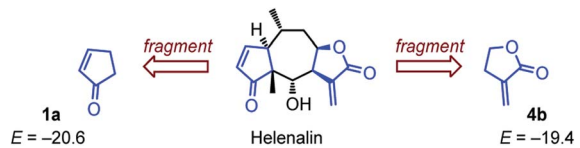

Fig. 10 Helenalin and individual reactivities of both electrophilic fragments.

Table 4 Experimental rate constants for the reactions of Michael acceptors **1–5** with GSH at 20 °C in aqueous solution, pH 7.4

Enone	Electrophilicity E	k_{GSH} (M^{-1} s^{-1})	k_2^{exp} (M^{-1} s^{-1})	$k_2^{exp}/k_2^{eqn\ (1)}$
1a	−20.6	$(9.34 \pm 0.66) \times 10^{-1}$, $(4.3 \times 10^{-1})^a$	33 (15)[a]	21 (9.3)[a]
1b	−22.1	3.33×10^{-3}[a]	0.12[a]	1/1.9[a]
2a	−22.1	$(1.18 \pm 0.07) \times 10^{-1}$, $(3.4 \times 10^{-1})^b$	4.2 (12)[b]	18 (52)[b]
4a	−20.7	$(1.93 \pm 0.09) \times 10^{-2}$	0.69	1/2.0
4b	−19.4	$(5.75 \pm 0.40) \times 10^{-1}$	21	2.8
5a	−21.8	$(1.77 \pm 0.17) \times 10^{-1}$	6.3	18
5b	−19.5	1.43 ± 0.11	51	7.7

[a] Calculated from kinetic data reported in ref. 19*d*. [b] Calculated from kinetic data in ref. 21*b*.

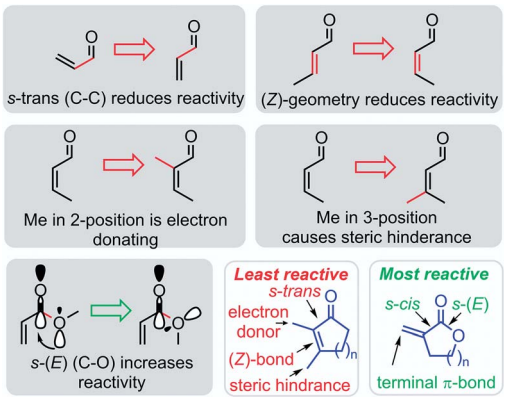

Fig. 11 Summary of stereoelectronic and steric effects on the electrophilic reactivity of cyclic enones and α,β-unsaturated lactones.

differences within one or two orders of magnitude are not unequivocally resolved by the simple three-parameter eqn (1). Changing the experimental method for determining the kinetics, swapping from a C- to an S-centered reference nucleophile as well as the neglect of constraint conformational space in natural products by the fragment approach may twist the relative reactivity order of similarly reactive Michael acceptors. Also the influence of solvents on the reactivity of carbonyl compounds needs further investigation.

The relative position of the lactone **5a** ($E = -21.8$) and (*E*)-pent-3-en-2-one ($E = -18.8$) or (*E*)-hex-4-en-3-one ($E = -18.9$) in the electrophilicity scale (Fig. 2) is in accord with the preferential binding of the ketone unit of rugulactone by nucleophilic sites in the course of covalent enzyme inhibition.[17] This illustrates that $\Delta E > 2.5$ enables a safe prognosis of the reactive site in a natural product with dual electrophilicity.

Conclusions

In summary, sulfonium and pyridinium ylides were utilized as one-bond reference nucleophiles in kinetic experiments to characterize the Mayr electrophilicity parameters *E* for various cyclic enones and α,β-unsaturated lactones in DMSO at 20 °C. By combining the electrophilicity parameters *E* with tabulated nucleophilicity descriptors *N* (and s_N) eqn (1) can be used to predict the rate constants for the reactions of **1–5** with various C-nucleophiles, as demonstrated by comparison with reported synthetic protocols.

Most valuable, the reactivities of cyclic core fragments of the Michael acceptors **1–5** agree with the observed electrophilicities of natural products (terpenes) of more complex structure and considerably higher molecular weight that contain the same reactive moiety. The distinct different reactivity of cyclic enones and unsaturated lactones compared to their acyclic analogs was analyzed by quantum-chemical calculations, distortion interaction analysis, and by considering stereoelectronic effects.

The most important structural effects on the reactivity of α,β-unsaturated carbonyl compounds are summarized in Fig. 11. The locked conformations of cyclic Michael acceptors have a significant impact on their electrophilic reactivities. If compared to analogous open-chain enones, the electrophilicity of cyclic enones is significantly reduced by the fixed (*Z*)-geometry of the *s-trans* configured π-system. Alkyl groups in either α- or β-position of the cyclic enones further attenuate the electrophilicity of cyclic enones by positive inductive effects and steric bulk in vicinity or directly at the electrophilic reaction center. Thus, β-alkylated cyclohexenones are among the least electrophilic species characterized so far in Mayr's reactivity scales.[24]

In contrast, the rigid cyclic structures of α-methylene-γ-butyrolactones facilitate synergistic stereoelectronic effects which favorably combine with a lack of steric hindrance at the reactive site to furnish a privileged class of highly potent electrophiles. In contrast to simple alkyl acrylates of comparable electrophilic reactivity, the cyclic scaffold of sesquiterpene lactones can be loaded with stereochemical information needed for recognition processes and selective reactions in living organisms. It is, therefore, not surprising that plants have chosen α-methylene-γ-butyrolactones as most abundant electrophilic fragment in biologically active sesquiterpene lactones.

The reactivity parameters determined in this work, together with those of previously characterized acyclic Michael acceptors, now provide an extensive basis for the systematic development of reactions with various classes of nucleophiles. Derivatization of natural products with the studied electron-deficient cyclic core fragments can in future be exploited in a more straightforward manner, thus saving limited natural resources, energy, and human effort. Knowledge of the electrophilic potential of these cyclic Michael acceptors to undergo

reactions with nucleophiles in combination with considering the thermodynamics of the intended reactions thus facilitates the rational design of synthesis with difficult to access and costly natural products and, in this way, fosters the development in discovery medicinal and pharmaceutical chemistry.

Conflicts of interest

There are no conflicts to declare.

Acknowledgements

The authors thank Prof. Herbert Mayr (LMU München) and Prof. Claude Y. Legault (Université de Sherbrooke) for helpful discussions. Financial support by the Deutsche Forschungsgemeinschaft (SFB 749, projects A3 and B1; OF 120/1-1, project number 410831260), the Fonds der Chemischen Industrie (Kekulé fellowship to RJM), the Department Chemie (LMU München), and the Department Chemie (TU München) is gratefully acknowledged.

Notes and references

1 *Sesquiterpene Lactones*, ed. V. P. Sülsen and V. S. Martino, Springer, Cham (CH), 2018.

2 J. A. Marco and M. Carda, in *Natural Lactones and Lactams: Synthesis, Occurrence and Biological Activity*, ed. T. Janecki, Wiley-VCH, Weinheim, 1st edn, 2014, ch. 2, pp. 51–100.

3 Ł. Albrecht, A. Albrecht and T. Janecki, in *Natural Lactones and Lactams: Synthesis, Occurrence and Biological Activity*, ed. T. Janecki, Wiley-VCH, Weinheim, 1st edn, 2014, ch. 4, pp. 147–192.

4 (*a*) M. H. Kunzmann, I. Staub, T. Böttcher and S. A. Sieber, *Biochemistry*, 2011, **50**, 910–916; (*b*) A. Janecka, A. Wyrebska, K. Gach, J. Fichna and T. Janecki, *Drug Discovery Today*, 2012, **17**, 561–572; (*c*) M. H. Kunzmann, N. C. Bach, B. Bauer and S. A. Sieber, *Chem. Sci.*, 2014, **5**, 1158–1167; (*d*) A. Coricello, J. D. Adams, E. J. Lien, C. Nguyen, F. Perri, T. J. Williams and F. Aiello, *Curr. Med. Chem.*, 2020, **27**, 1501–1514; (*e*) R. R. A. Freund, P. Gobrecht, D. Fischer and H.-D. Arndt, *Nat. Prod. Rep.*, 2020, **37**, 541–565.

5 (*a*) A. Ghantous, A. Sinjab, Z. Herceg and N. Darwiche, *Drug Discovery Today*, 2013, **18**, 894–905; (*b*) C. A. Berdan, R. Ho, H. S. Lehtola, M. To, X. Hu, T. R. Huffman, Y. Petri, C. R. Altobelli, S. G. Demeulenaere, J. A. Olzmann, T. J. Maimone and D. K. Nomura, *Cell Chem. Biol.*, 2019, **26**, 1027–1035; (*c*) J. N. Spradlin, X. Hu, C. C. Ward, S. M. Brittain, M. D. Jones, L. Ou, M. To, A. Proudfoot, E. Ornelas, M. Woldegiorgis, J. A. Olzmann, D. E. Bussiere, J. R. Thomas, J. A. Tallarico, J. M. McKenna, M. Schirle, T. J. Maimone and D. K. Nomura, *Nat. Chem. Biol.*, 2019, **15**, 747–755.

6 P. A. Jackson, J. C. Widen, D. A. Harki and K. M. Brummond, *J. Med. Chem.*, 2017, **60**, 839–885.

7 (*a*) J. Krysiak and R. Breinbauer, *Top. Curr. Chem.*, 2012, **324**, 43–84; (*b*) R. Lagoutte and N. Winssinger, *Chimia*, 2017, **71**, 703–711; (*c*) D. K. Nomura and T. J. Maimone, in *Activity-Based Protein Profiling (Curr. Top. Microbiol. Immun., vol. 420)*, ed. B. F. Cravatt, K.-L. Hsu and E. Weerapana, Springer, Cham (CH), 2018; pp. 351–374, DOI: 10.1007/82_2018_121.

8 P. E. Ordóñez, K. K. Sharma, L. M. Bystrom, M. A. Alas, R. G. Enriquez, O. Malagón, D. E. Jones, M. L. Guzman and C. M. Compadre, *J. Nat. Prod.*, 2016, **79**, 691–696.

9 (*a*) S. M. Kupchan, D. C. Fessler, M. A. Eakin and T. J. Giacobbe, *Science*, 1970, **168**, 376–377; (*b*) R. R. A. Kitson, A. Millemaggi and R. J. K. Taylor, *Angew. Chem., Int. Ed.*, 2009, **48**, 9426–9451.

10 Q. Li, Z. Wang, Y. Xie and H. Hu, *Biomed. Pharmacother.*, 2020, **125**, 109955.

11 (*a*) N. Kudo, N. Matsumori, H. Taoka, D. Fujiwara, E. P. Schreiner, B. Wolff, M. Yoshida and S. Horinouchi, *Proc. Natl. Acad. Sci. U. S. A.*, 1999, **96**, 9112–9117; (*b*) Q. Sun, Y. P. Carrasco, Y. Hu, X. Guo, H. Mirzaei, J. MacMillan and Y. M. Chook, *Proc. Natl. Acad. Sci. U. S. A.*, 2013, **110**, 1303–1308.

12 S. B. Buck, C. Hardouin, S. Ichikawa, D. R. Soenen, C.-M. Gauss, I. Hwang, M. R. Swingle, K. M. Bonness, R. E. Honkanen and D. L. Boger, *J. Am. Chem. Soc.*, 2003, **125**, 15694–15695.

13 T. J. Schmidt, in *Studies in Natural Products Chemistry*, ed. Atta-ur-Rahman, Elsevier, Amsterdam, 2006, vol. 33, pp. 309–392.

14 T. J. Schmidt, in *Sesquiterpene Lactones*, ed. V. P. Sülsen, V. S. Martino, Springer, Cham (CH), 2018, ch. 15, pp. 349–371.

15 E. A. Crane and K. Gademann, *Angew. Chem., Int. Ed.*, 2016, **55**, 3882–3902.

16 J.-T. Feng, D.-L. Wang, Y.-L. Wu, Y. He and Z. Xing, *Bioorg. Med. Chem. Lett.*, 2013, **23**, 4393–4397.

17 M. B. Nodwell, H. Menz, S. F. Kirsch and S. A. Sieber, *ChemBioChem*, 2012, **13**, 1439–1446.

18 (*a*) X. Li, D. T. Payne, B. Ampolu, N. Bland, J. T. Brown, M. J. Dutton, C. A. Fitton, A. Gulliver, L. Hale, D. Hamza, G. Jones, R. Lane, A. G. Leach, L. Male, E. G. Merisor, M. J. Morton, A. S. Quy, R. Roberts, R. Scarll, T. Schulz-Utermoehl, T. Stankovic, B. Stevenson, J. S. Fossey and A. Agathanggelou, *MedChemComm*, 2019, **10**, 1379–1390; (*b*) C. Tian, R. Sun, K. Liu, L. Fu, X. Liu, W. Zhou, Y. Yang and J. Yang, *Cell Chem. Biol.*, 2017, **24**, 1416–1427.

19 (*a*) T. W. Schultz, J. W. Yarbrough and E. L. Johnson, *SAR QSAR Environ. Res.*, 2005, **16**, 313–322; (*b*) J. W. Yarbrough and T. W. Schultz, *Chem. Res. Toxicol.*, 2007, **20**, 558–562; (*c*) A. Böhme, D. Thaens, A. Paschke and G. Schüürmann, *Chem. Res. Toxicol.*, 2009, **22**, 742–750; (*d*) A. Böhme, A. Laqua and G. Schüürmann, *Chem. Res. Toxicol.*, 2016, **29**, 952–962.

20 V. J. Cee, L. P. Volak, Y. Chen, M. D. Bartberger, C. Tegley, T. Arvedson, J. McCarter, A. S. Tasker and C. Fotsch, *J. Med. Chem.*, 2015, **58**, 9171–9178.

21 (*a*) M. Friedman, J. F. Cavins and J. S. Wall, *J. Am. Chem. Soc.*, 1965, **87**, 3672–3682; (*b*) H. Esterbauer, H. Zollner and N. Scholz, *Z. Naturforsch., C: J. Biosci.*, 1975, **30**, 466–473.

22 (*a*) G. Eisenbrand, J. Schuhmacher and P. Gölzer, *Chem. Res. Toxicol.*, 1995, **8**, 40–46; (*b*) K. Chan, R. Poon and P. J. O'Brien, *J. Appl. Toxicol.*, 2008, **28**, 1027–1039.

23 J. A. H. Schwöbel, D. Wondrousch, Y. K. Koleva, J. C. Madden, M. T. D. Cronin and G. Schüürmann, *Chem. Res. Toxicol.*, 2010, **23**, 1576–1585.

24 (*a*) H. Mayr and M. Patz, *Angew. Chem., Int. Ed. Engl.*, 1994, **33**, 938–957; (*b*) H. Mayr, T. Bug, M. F. Gotta, N. Hering, B. Irrgang, B. Janker, B. Kempf, R. Loos, A. R. Ofial, G. Remennikov and H. Schimmel, *J. Am. Chem. Soc.*, 2001, **123**, 9500–9512; (*c*) H. Mayr and A. R. Ofial, *SAR QSAR Environ. Res.*, 2015, **26**, 619–646; (*d*) The database of reactivity parameters (E, N, and s_N) is freely accessible under, www.cup.lmu.de/oc/mayr/reaktionsdatenbank2/, accessed Jan., 2021.

25 R. J. Mayer and A. R. Ofial, *Angew. Chem., Int. Ed.*, 2019, **58**, 17704–17708.

26 Q. Chen, P. Mayer and H. Mayr, *Angew. Chem., Int. Ed.*, 2016, **55**, 12664–12667.

27 D. S. Allgäuer, H. Jangra, H. Asahara, Z. Li, Q. Chen, H. Zipse, A. R. Ofial and H. Mayr, *J. Am. Chem. Soc.*, 2017, **139**, 13318–13329.

28 A. Kakehi, *Heterocycles*, 2012, **85**, 1529–1577.

29 D. S. Allgäuer and H. Mayr, *Eur. J. Org. Chem.*, 2013, 6379–6388 and ref. cited therein.

30 D. S. Allgäuer and H. Mayr, *J. Am. Chem. Soc.*, 2013, **135**, 15216–15224.

31 D. S. Allgäuer and H. Mayr, *Eur. J. Org. Chem.*, 2014, 2956–2963.

32 Y. Tamura, Y. Sumida, S.-I. Haruki and M. Ikeda, *J. Chem. Soc., Perkin Trans. 1*, 1975, 575–579.

33 R.-B. Hu, S. Sun and Y. Su, *Angew. Chem., Int. Ed.*, 2017, **56**, 10877–10880.

34 T. Zincke and H. Rollhäuser, *Chem. Ber.*, 1912, **45**, 1495–1511.

35 F. von Nussbaum, V. M.-J. Li, S. Allerheiligen, S. Anlauf, L. Bärfacker, M. Bechem, M. Delbeck, M. F. Fitzgerald, M. Gerisch, H. Gielen-Haertwig, H. Haning, D. Karthaus, D. Lang, K. Lustig, D. Meibom, J. Mittendorf, U. Rosentreter, M. Schäfer, S. Schäfer, J. Schamberger, L. A. Telan and A. Tersteegen, *ChemMedChem*, 2015, **10**, 1163–1173.

36 (*a*) V. K. Aggarwal, H. W. Smith, G. Hynd, R. V. H. Jones, R. Fieldhouse and S. E. Spey, *J. Chem. Soc., Perkin Trans. 1*, 2000, 3267–3276; (*b*) M. Liao, L. Peng and J. Wang, *Org. Lett.*, 2008, **10**, 693–696.

37 R. Appel, N. Hartmann and H. Mayr, *J. Am. Chem. Soc.*, 2010, **132**, 17894–17900.

38 R. Huisgen, *Angew. Chem., Int. Ed.*, 1970, **9**, 751–762.

39 A. Otto, B. Abegaz, B. Ziemer and J. Liebscher, *Tetrahedron: Asymmetry*, 1999, **10**, 3381–3389.

40 E. S. Beh, L. Tong and R. G. Gordon, *Organometallics*, 2017, **36**, 1453–1456.

41 J.-C. Le Menn, A. Tallec and J. Sarrazin, *Can. J. Chem.*, 1991, **69**, 761–767.

42 N. Martin-Leon, M. Quinteiro, C. Seoane and J. L. Soto, *Liebigs Ann. Chem.*, 1990, 101–104.

43 C. Bigogno, B. Danieli, G. Lesma and D. Passarella, *Heterocycles*, 1995, **41**, 973–982.

44 D. M. Altshuler, C. D. Anderson, W. G. Chen, J. J. Clemens, T. Cleveland, T. R. Coon, B. Frieman, P. Grootenhuis, S. S. Hadida Ruah, B. J. Hare, R. Kewalramani, J. Mccartney, M. T. Miller, P. Paraselli, F. Pierre, S. M. Robertson, P. R. Sosnay, S. E. Swift and J. Zhou, WO 2020/102346A1, Vertex Pharmaceutical Inc., 2020, p. 46.

45 K. E. Bailey and B. R. Davis, *Aust. J. Chem.*, 1995, **48**, 1827–1834.

46 K. Dudzinski, A. M. Pakulska and P. Kwiatkowski, *Org. Lett.*, 2012, **14**, 4222–4225.

47 (*a*) M. Puppala, A. Murali and S. Baskaran, *Chem. Commun.*, 2012, **48**, 5778–5780; (*b*) H. O. House, W. A. Kleschick and E. J. Zaiko, *J. Org. Chem.*, 1978, **43**, 3653–3661.

48 (*a*) J. Cossy, N. Furet and S. BouzBouz, *Tetrahedron*, 1995, **51**, 11751–11764; (*b*) P. J. Crowley, I. H. Aspinall, K. Gillen, C. R. A. Godfrey, I. M. Devillers, G. R. Munns, O.-A. Sageot, J. Swanborough, P. A. Worthington and J. Williams, *Chimia*, 2003, **57**, 685–691.

49 R. González, I. Collado, B. López de Uralde, A. Marcos, L. M. Martín-Cabrejas, C. Pedregal, J. Blanco-Urgoiti, J. Pérez-Castells, M. A. Fernández, S. L. Andis, B. G. Johnson, R. A. Wright, D. D. Schoepp and J. A. Monn, *Bioorg. Med. Chem.*, 2005, **13**, 6556–6570.

50 I. Collado, C. Pedregal, A. B. Bueno, A. Marcos, R. González, J. Blanco-Urgoiti, J. Pérez-Castells, D. D. Schoepp, R. A. Wright, B. G. Johnson, A. E. Kingston, E. D. Moher, D. W. Hoard, K. I. Griffey and J. P. Tizzano, *J. Med. Chem.*, 2004, **47**, 456–466.

51 R. Gnaneshwar and S. Sivaram, *Synth. Commun.*, 2006, **36**, 885–890.

52 S. Kawanishi, K. Sugiyama, Y. Oki, T. Ikawa and S. Akai, *Green Chem.*, 2017, **19**, 411–417.

53 S. J. Robbins and D. M. S. Wheeler, *Synth. Commun.*, 1989, **19**, 769–775.

54 B. R. Davis, S. R. Gupta and T. G. Halsall, *J. Chem. Soc.*, 1961, 4211–4214.

55 (*a*) M.-A. Poupart, G. Lassalle and L. A. Paquette, *Org. Synth.*, 1990, **69**, 173; (*b*) W. G. Dauben and J. M. Gerdes, *Tetrahedron Lett.*, 1983, **24**, 3841–3844.

56 (*a*) R. Sauvetre, M.-C. Roux-Schmitt and J. Seyden-Penne, *Tetrahedron*, 1978, **34**, 2135–2140; (*b*) M.-C. Roux-Schmitt, L. Wartski and J. Seyden-Penne, *Synth. Commun.*, 1981, **11**, 85–94.

57 (*a*) A. V. Marenich, C. J. Cramer and D. G. Truhlar, *J. Phys. Chem. B*, 2009, **113**, 6378–6396; (*b*) Y. Zhao and D. G. Truhlar, *Theor. Chem. Acc.*, 2008, **120**, 215–241; (*c*) M. J. Frisch, G. W. Trucks, H. B. Schlegel, G. E. Scuseria, M. A. Robb, J. R. Cheeseman, G. Scalmani, V. Barone, G. A. Petersson, H. Nakatsuji, X. Li, M. Caricato, A. V. Marenich, J. Bloino, B. G. Janesko, R. Gomperts, B. Mennucci, H. P. Hratchian, J. V. Ortiz, A. F. Izmaylov, J. L. Sonnenberg, D. Williams-Young, F. Ding, F. Lipparini, F. Egidi, J. Goings, B. Peng, A. Petrone, T. Henderson, D. Ranasinghe, V. G. Zakrzewski, J. Gao, N. Rega, G. Zheng, W. Liang, M. Hada, M. Ehara, K. Toyota,

R. Fukuda, J. Hasegawa, M. Ishida, T. Nakajima, Y. Honda, O. Kitao, H. Nakai, T. Vreven, K. Throssell, J. A. Montgomery Jr, J. E. Peralta, F. Ogliaro, M. J. Bearpark, J. J. Heyd, E. N. Brothers, K. N. Kudin, V. N. Staroverov, T. A. Keith, R. Kobayashi, J. Normand, K. Raghavachari, A. P. Rendell, J. C. Burant, S. S. Iyengar, J. Tomasi, M. Cossi, J. M. Millam, M. Klene, C. Adamo, R. Cammi, J. W. Ochterski, R. L. Martin, K. Morokuma, O. Farkas, J. B. Foresman and D. J. Fox, *Gaussian 16, Revision A.03*, Gaussian, Inc., Wallingford CT, 2016; (*d*) C. Y. Legault, *CYLview 1.0b*, Université de Sherbrooke, 2009, http://www.cylview.org.

58 A. Bienvenüe, *J. Am. Chem. Soc.*, 1973, **95**, 7345–7353.

59 H. K. Hall Jr, M. K. Brandt and R. M. Mason, *J. Am. Chem. Soc.*, 1958, **80**, 6420–6427.

60 (*a*) R. Huisgen, *Angew. Chem.*, 1957, **69**, 341–359; (*b*) R. Huisgen and H. Ott, *Tetrahedron*, 1959, **6**, 253–267.

61 I. Alabugin, *Stereoelectronic Effects: A Bridge Between Structure and Reactivity*, Wiley, Chichester (UK), 2016, ch. 6, pp. 149–150.

62 (*a*) D. H. Ess and K. N. Houk, *J. Am. Chem. Soc.*, 2007, **129**, 10646–10647; (*b*) D. H. Ess and K. N. Houk, *J. Am. Chem. Soc.*, 2008, **130**, 10187–10198; (*c*) Y. Lan, L. Zou, Y. Cao and K. N. Houk, *J. Phys. Chem. A*, 2011, **115**, 13906–13920; (*d*) F. M. Bickelhaupt and K. N. Houk, *Angew. Chem., Int. Ed.*, 2017, **56**, 10070–10086; (*e*) P. Vermeeren, S. C. C. van der Lubbe, C. F. Guerra, F. M. Bickelhaupt and T. A. Hamlin, *Nat. Protoc.*, 2020, **15**, 649–667.

63 J. Hine, *Adv. Phys. Org. Chem.*, 1977, **15**, 1–61.

64 (*a*) B. Jeziorski, R. Moszynski and K. Szalewicz, *Chem. Rev.*, 1994, **94**, 1887–1930; (*b*) T. M. Parker, L. A. Burns, R. M. Parrish, A. G. Ryno and C. D. Sherrill, *J. Chem. Phys.*, 2014, **140**, 094106; (*c*) R. M. Parrish, L. A. Burns, D. G. A. Smith, A. C. Simmonett, A. E. DePrince III, E. G. Hohenstein, U. Bozkaya, A. Yu. Sokolov, R. Di Remigio, R. M. Richard, J. F. Gonthier, A. M. James, H. R. McAlexander, A. Kumar, M. Saitow, X. Wang, B. P. Pritchard, P. Verma, H. F. Schaefer III, K. Patkowski, R. A. King, E. F. Valeev, F. A. Evangelista, J. M. Turney, T. D. Crawford and C. D. Sherrill, *J. Chem. Theory Comput.*, 2017, **13**, 3185–3197.

65 Pyramidalization Δ in the transition states of the reactions of **7** with the cyclohexenones **2a**, **2b**, and **2c** follows an analogous pattern as discussed for the cyclopentenones, that is, decreasing electrophilic reactivity is correlated with increasing pyramidalization Δ (see ESI, Table S1†).

66 Presumably due to the very small differences in the interaction energies, SAPT analysis of the reaction pathways of the reactions of **7** with **1a** and **1b** did not provide sufficient insight to reveal the underlying reasons for the difference in interaction energies (see ESI, Fig. S2†).

67 G. Lyss, T. J. Schmidt, I. Merfort and H. L. Pahl, *Biol. Chem.*, 1997, **378**, 951–961.

68 (*a*) T. J. Schmidt, *Bioorg. Med. Chem.*, 1997, **5**, 645–653; (*b*) T. J. Schmidt, G. Lyß, H. L. Pahl and I. Merfort, *Bioorg. Med. Chem.*, 1999, **7**, 2849–2855.

69 (*a*) J. C. Widen, A. M. Kempema, J. W. Baur, H. M. Skopec, J. T. Edwards, T. J. Brown, D. A. Brown, F. A. Meece and D. A. Harki, *ChemMedChem*, 2018, **13**, 303–311; (*b*) In this work, we observed a half-life time of the **1a**-GSH adduct of $t_{1/2}$ = 40 min (under the conditions of the kinetic GSH chemoassay).